SINTEF
PROCEEDINGS
2

Proceedings of the 12th International Conference on Computational Fluid Dynamics in the Oil & Gas, Metallurgical and Process Industries

Progress in Applied CFD – CFD2017

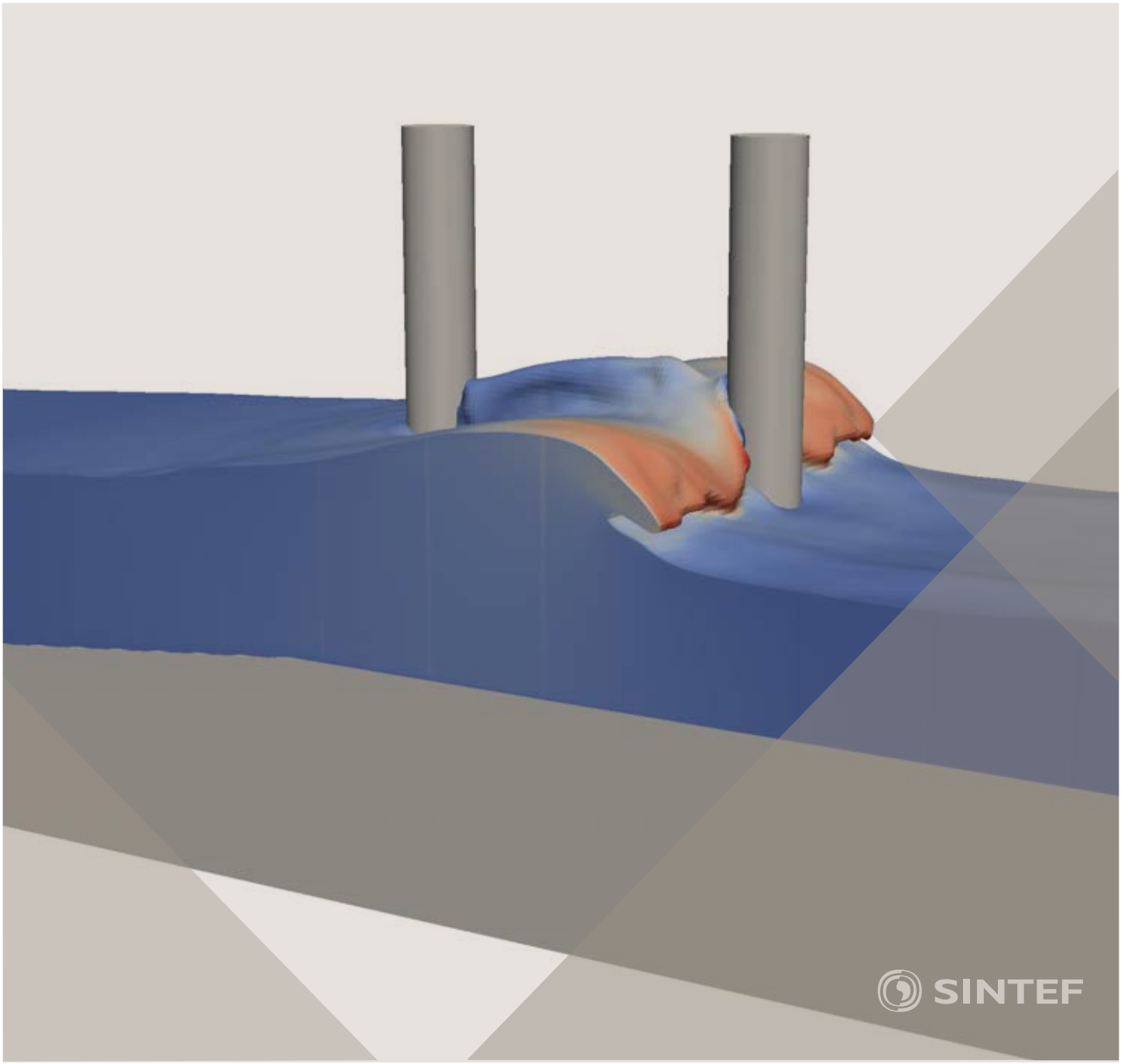

SINTEF Proceedings

Editors:
Jan Erik Olsen and Stein Tore Johansen

Progress in Applied CFD – CFD2017

Proceedings of the 12th International Conference on Computational Fluid Dynamics in the Oil & Gas, Metallurgical and Process Industries

SINTEF Academic Press

SINTEF Proceedings no 2
Editors: Jan Erik Olsen and Stein Tore Johansen
Progress in Applied CFD – CFD2017
Selected papers from 10th International Conference on Computational Fluid Dynamics in the Oil & Gas, Metallurgical and Process Industries

Key words:
CFD, Flow, Modelling

Cover, illustration: Arun Kamath

ISSN 2387-4295 (online)
ISBN 978-82-536-1544-8 (pdf)

SINTEF Academic Press
Address: Forskningsveien 3 B
PO Box 124 Blindern
N-0314 OSLO
Tel: +47 73 59 30 00
Fax: +47 22 96 55 08

www.sintef.no/byggforsk
www.sintefbok.no

SINTEF Proceedings
SINTEF Proceedings is a serial publication for peer-reviewed conference proceedings on a variety of scientific topics.
The processes of peer-reviewing of papers published in SINTEF Proceedings are administered by the conference organizers and proceedings editors. Detailed procedures will vary according to custom and practice in each scientific community.

PREFACE

This book contains all manuscripts approved by the reviewers and the organizing committee of the 12th International Conference on Computational Fluid Dynamics in the Oil & Gas, Metallurgical and Process Industries. The conference was hosted by SINTEF in Trondheim in May/June 2017 and is also known as CFD2017 for short. The conference series was initiated by CSIRO and Phil Schwarz in 1997. So far the conference has been alternating between CSIRO in Melbourne and SINTEF in Trondheim. The conferences focuses on the application of CFD in the oil and gas industries, metal production, mineral processing, power generation, chemicals and other process industries. In addition pragmatic modelling concepts and bio-mechanical applications have become an important part of the conference. The papers in this book demonstrate the current progress in applied CFD.

The conference papers undergo a review process involving two experts. Only papers accepted by the reviewers are included in the proceedings. 108 contributions were presented at the conference together with six keynote presentations. A majority of these contributions are presented by their manuscript in this collection (a few were granted to present without an accompanying manuscript).

The organizing committee would like to thank everyone who has helped with review of manuscripts, all those who helped to promote the conference and all authors who have submitted scientific contributions. We are also grateful for the support from the conference sponsors: ANSYS, SFI Metal Production and NanoSim.

Stein Tore Johansen & Jan Erik Olsen

Organizing committee:

Conference chairman: Prof. Stein Tore Johansen
Conference coordinator: Dr. Jan Erik Olsen
Dr. Bernhard Müller
Dr.Sigrid Karstad Dahl
Dr.Shahriar Amini
Dr.Ernst Meese
Dr.Josip Zoric
Dr.Jannike Solsvik
Dr.Peter Witt

Scientific committee:

Stein Tore Johansen, SINTEF/NTNU
Bernhard Müller, NTNU
Phil Schwarz, CSIRO
Akio Tomiyama, Kobe University
Hans Kuipers, Eindhoven University of Technology
Jinghai Li, Chinese Academy of Science
Markus Braun, Ansys
Simon Lo, CD-adapco
Patrick Segers, Universiteit Gent
Jiyuan Tu, RMIT
Jos Derksen, University of Aberdeen
Dmitry Eskin, Schlumberger-Doll Research
Pär Jönsson, KTH
Stefan Pirker, Johannes Kepler University
Josip Zoric, SINTEF

CONTENTS

MULTIPHASE DIRECT NUMERICAL SIMULATIONS (DNS) OF OIL-WATER FLOWS THROUGH HOMOGENEOUS POROUS ROCKS

H.V. PATEL[1]*, **J.A.M. KUIPERS**[1], **E.A.J.F. PETERS**[1]

[1]Multiphase Reactors Group, Dept. of Chemical Engineering and Chemistry, Eindhoven University of Technology, P.O. Box 513, 5600 MB Eindhoven, THE NETHERLANDS

* E-mail: h.v.patel@tue.nl

ABSTRACT

Water flooding is commonly used to recover oil from porous rocks using pressurized water. Present study focuses on fully resolved pore-scale level multiphase Direct Numerical Simulations (DNS) of oil-water flows through homogeneous porous rocks. A second order accurate implicit Immersed Boundary Method (IBM) is used to resolve fluid-solid interactions on a non-body fitted Cartesian computational grid. Dynamic evolution of the fluid-fluid interface is tracked by a mass conservative sharp interface Volume of Fluid (VOF) method. The IBM and VOF method are coupled by a prescribed contact angle boundary condition at the fluid-fluid-solid contact line. Our method has been extensively validated especially for the test cases involving oil-water flows. Simulations of water flooding process through periodic homogeneous configurations of spheres are performed based on typical pore-scale capillary and Reynolds numbers. Effect of wettability on the mobility of oil through oil-wet and neutrally-wet rocks has been quantified as well.

Keywords: water flooding, porous rocks, Immersed Boundary Method (IBM), Volume of Fluid (VOF), contact angle .

NOMENCLATURE

Notations

p	Pressure, $[Pa]$
F	Fluid phase fraction, $[-]$
M	Dynamic viscosity ratio, $[-]$
Re	Reynolds number, $[-]$
Ca	Capillary number, $[-]$
S	Fluid phase saturation, $[-]$
k	Permeability, $[m^2]$
x	x co-ordinate, $[m]$
y	y co-ordinate, $[m]$
z	z co-ordinate, $[m]$

Greek Symbols

ρ	Mass density, $[kg/m^3]$
μ	Dynamic viscosity, $[Pa \cdot s]$
σ	Surface tension, $[N/m]$
Δ	Grid size, $[m]$
θ	(Static) contact angle, $[degree]$
ϕ	Porosity, $[-]$

Vectors

$\mathbf{u}$	Velocity, $[m/s]$
$\mathbf{F}_\sigma$	Surface tension force, $[N]$
$\mathbf{g}$	Gravitational acceleration, $[m/s^2]$

Sub/superscripts

$1,2$	Fluid phase number
w	Wetting fluid
nw	Non-wetting fluid

INTRODUCTION

Multiphase flows in complex structures are encountered widely in nature and technology. One such example is water flooding (Sheng, 2014) used for oil recovery. After the primary (natural) recovery of the oil from reservoir, large amount of oil remains trapped in the porous rocks. Secondary and ternary recovery processes (e.g. water flooding, gas injection, thermal processes, chemical flooding etc.) are then used for further recovery of such residual oil. In water flooding high pressure and/or high temperature water is pushed through porous rocks which carries oil out of the porous bed. Focus of the current work is to perform pore-scale simulations of oil-water multiphase flows through complex rock structures during such a water flooding process. To serve this purpose, three different problems need to be tackled: i) oil-water multi-fluid interface tracking, ii) interactions between fluids (oil or water) and complex solid geometries, and iii) three-phase contact line dynamics.

A wide range of numerical methods (e.g. Front Tracking, Volume of Fluid, Level Set etc.) has been developed and tested successfully to track multi-fluid interfaces (Wörner, 2003). They all differ with respect to tackling the following complexity: i) interface advection based on local velocity field and ii) surface tension force based on local interface curvature. The volume of fluid (VOF) method (Hirt and Nichols, 1981; Youngs, 1982) uses a color function F which denotes the local fluid phase fraction in the immiscible mixture of fluids. Advection of F is governed by pseudo-Lagrangian geometrical advection schemes to minimize numerical diffusion. This particular feature makes VOF the most mass conservative among all multi-fluid interface tracking methods. The density-scaled continuum surface force (CSF) model proposed by Brackbill *et al.* (1992) is used to evaluate the surface tension force for its simplicity and robustness especially in the presence of complex solid boundaries.

The immersed boundary method (IBM) (Mittal and Iaccarino, 2005) is a set of computational techniques which

uses non-body fitted (mainly Cartesian) grids for simulating fluid-solid interactions through complex geometries. It eliminates the need of traditional unstructured body fitted grids and hence provides simplicity in grid generation and discretization, ease of code development, less memory requirement and higher computational efficiency. A direct forcing approach used in IBM produces a sharp fluid-solid interface without spatial spreading. So, in the present work a direct forcing, implicit, second order IBM (Deen *et al.*, 2012; Das *et al.*, 2016) is used which does not require any calibration for the different complex geometries.

Fluid-fluid interfaces in contact with solid boundaries produce a three-phase contact line. The contact line behavior is determined by microscopic physicochemical interactions between molecules of two different immiscible fluids and the solid substrate, and it can drastically affect the statics and dynamics of the bulk flow (Snoeijer and Andreotti, 2013). An apparent contact angle at the macroscopic length scales is a result of these microscopic interactions at the contact line. In the present work, a coupled IBM-VOF method has been used to simulate contact line dynamics.

This paper deals with validation/verification and application of the developed IBM-VOF solver specifically for multiphase flows involving oil and water. It is organized as follows: We first describe the governing Navier-Stokes equations for multiphase flows along with the F-advection equation. Next, we discuss numerical and implementation details in brief. Further, the coupled IBM-VOF solver is extensively validated/verified for the test cases involving oil-water flows. Last, a water flooding process is simulated on the pore-scale and the effect of wettability on the mobility of oil has been quantified for oil-wet and neutrally-wet homogeneous rocks.

MODEL DESCRIPTION

Governing equations

For incompressible multiphase flows the Navier-Stokes equations can be combined into a single equation for $\mathbf{u}$ in the entire domain. Surface tension due to the presence of a curved deformable fluid-fluid interface is taken into account by a local volumetric $\mathbf{F}_\sigma$. The governing mass and momentum conservation equations for unsteady, incompressible, Newtonian, multiphase flows are expressed as follows:

$$\nabla \cdot \mathbf{u} = 0 \tag{1}$$

$$\rho \frac{\partial \mathbf{u}}{\partial t} + \rho \nabla \cdot (\mathbf{u}\mathbf{u}) = -\nabla p + \nabla \cdot \boldsymbol{\tau} + \rho \mathbf{g} + \mathbf{F}_\sigma \tag{2}$$

where $\boldsymbol{\tau} = \mu[\nabla \mathbf{u} + (\nabla \mathbf{u})^T]$ is the fluid stress tensor. Advection of F is governed by the following equation:

$$\frac{DF}{Dt} = \frac{\partial F}{\partial t} + \mathbf{u} \cdot \nabla F = 0 \tag{3}$$

This equation expresses that the interface is advected with the local fluid velocity. To evaluate the local averaged density, linear averaging of the densities of the fluid 1 $(F = 1)$ and fluid 2 $(F = 0)$ is used:

$$\rho = F\rho_1 + (1 - F)\rho_2 \tag{4}$$

Similarly, the local average μ could also be evaluated by linear averaging of the dynamic viscosities of individual fluid phase. Alternatively, following a fundamental approach proposed by Prosperetti (2002), the local average kinematic viscosity is evaluated by harmonic averaging of the kinematic viscosities of the individual fluid phases:

$$\frac{\rho}{\mu} = F\frac{\rho_1}{\mu_1} + (1 - F)\frac{\rho_2}{\mu_2} \tag{5}$$

In all the computations reported in this paper, Eq. (4) and Eq. (5) are used to evaluate the local average density and dynamic viscosity, respectively.

Numerical and Implementation Details

In the current implementation, the finite volume method is used to solve the mass and momentum conservation equations in each control volume of a staggered computational grid. To simulate multiphase flows involving multi fluid-solid interactions three things need to be dealt with: i) dynamic interactions between fluids and non-deformable solids, ii) dynamics of deformable fluid-fluid interfaces, and iii) contact line dynamics at the three phase contact lines.

An implicit (direct) second-order accurate IBM proposed by Deen *et al.* (2012) and described in detail by Das *et al.* (2016) has been used to apply no-slip boundary conditions for fluids-solid interactions at immersed boundaries. VOF (Van Sint Annaland *et al.*, 2005) to track fluid-fluid interface consists of three main parts: i) solution of F-advection equation, ii) computation of the volumetric $\mathbf{F}_\sigma$, and iii) smoothing of F. In presence of fluid-fluid interfaces with immersed solids, contact line dynamics plays a major role in wetting-dewetting phenomena. It is incorporated in our coupled IBM-VOF framework (Patel *et al.*, 2017) by applying the apparent contact angle as a boundary condition at contact lines. The contact angle may have a single value (static) or different values (dynamic) depending upon the local contact parameters and fluid properties. The effect of the contact angle is taken into account by modifying the interface normals at the solid boundaries. Readers may refer to the mentioned literature for intrinsic numerical and implementation details.

VERIFICATION AND VALIDATION

The IBM and VOF implementations have been tested individually by Das *et al.* (2016) and Van Sint Annaland *et al.* (2005) respectively for various cases and they obtained excellent agreement with numerical and experimental results published in literature. The 3D coupled IBM-VOF implementation with contact line dynamics has been validated by Patel *et al.* (2017) with static and/or dynamic contact angles for i) the equilibrium shape of a droplet on a flat surface, ii) the equilibrium shape of a droplet on a spherical surface, and iii) temporal evolution of droplet contact radius on flat surface (generated with and without IBM).

In this section, we investigate additional validation/verification test cases specifically addressing the oil-water multiphase flows. First, a test case of 2D multiphase Poiseuille flow is considered to compare the velocity profiles and relative permeabilities with analytical expressions. Further, a viscous fingering phenomenon is simulated in a 2D channel and finger characteristics parameters i.e. dimensionless finger width and tip radius have been compared with results published in literature. Last, a grid independence study for the contact force is presented for 3D coupled IBM-VOF implementation.

2D Multiphase Poiseuille Flow

In this section, we investigate the co-current multiphase Poiseuille flow of two immiscible fluids namely wetting and non-wetting fluid. The wetting fluid is in contact with the channel walls ($a < |y| < L$) whereas the non-wetting fluid resides between the layers of wetting fluid ($0 < |y| < a$) as shown in Figure 1. No-slip boundary conditions are applied at the

channel walls ($|y| = L$) and the flow in x-direction is periodic. Both fluids have the same density ($\rho_w = \rho_{nw}$) and different dynamic viscosities giving the definition of $M = \mu_{nw}/\mu_w$. A constant body force G is applied to both fluids in the x-direction such as the flow remains in the Stokes regime ($Re << 1$). Due to the existence of a flat fluid-fluid interface, the surface tension force doesn't play any role in this problem.

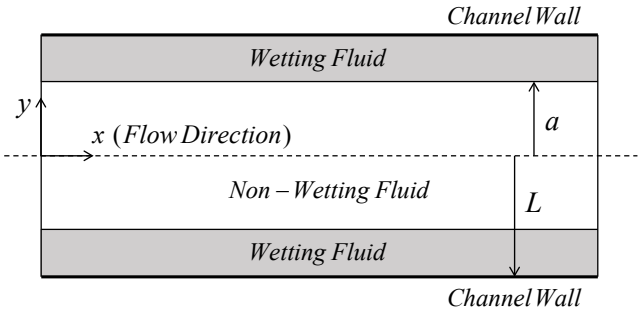

Figure 1: Schematic diagram of 2D multiphase Poiseuille flow.

For the given value of wetting and non-wetting saturation ($S_w = (1-a)/L$ and $S_{nw} = a/L$), the analytical expressions for the velocity of the wetting and non-wetting fluids (u_w and u_{nw}) are given by:

$$\begin{aligned} u_w(y) &= \frac{G}{2\mu_w}(L^2 - y^2) \\ u_{nw}(y) &= \frac{G}{2\mu_w}(L^2 - a^2) + \frac{G}{2\mu_{nw}}(a^2 - y^2) \end{aligned} \tag{6}$$

Similarly, the analytical expressions for the relative permeability of each fluid ($k_{r,w}$ and $k_{r,nw}$) can be given as,

$$\begin{aligned} k_{r,w} &= \frac{1}{2}S_w^2(3 - S_w) \\ k_{r,nw} &= S_{nw}\left[\frac{3}{2}M + S_{nw}^2\left(1 - \frac{3}{2}M\right)\right] \end{aligned} \tag{7}$$

Readers are referred to Yiotis *et al.* (2007) for the detailed derivation of Equation (6) and (7). Equation (7) suggests that $k_{r,w}$ is always bounded between 0 to 1 as it is only function of S_w. However, $k_{r,nw}$ may become greater than 1 in case $M > 1$ due to the 'lubricating' effect of the wetting fluid.

Simulations have been performed for $M = 0.01, 1$ and 100 with S_w ranging from 0 to 1 with increment of 0.1. Total 100 grid cells have been taken across L. Figure 2 shows analytical and numerical velocity profiles for the case of $M = 100$ and $S_w = 0.5$. Figure 3 compares analytical and numerical relative permeabilities for wetting and non-wetting fluids for $M = 100$. Our simulations show an excellent agreement with analytical results having maximum error in relative permeability to be less than 0.2%. Huang and Lu (2009) reports this error to be nearly 7% using multiphase Lattice-Boltzmann method. Also, in their results, continuity of the shear stress is not maintained at the interface and hence a velocity jump is observed.

Viscous Finger in a 2D Channel

A viscous finger is an instability that may occur when a low viscosity fluid displaces high viscosity fluid. In this section, we simulate the single viscous finger formation phenomenon in a 2D channel. Initially, a channel with finite width H is fully saturated with high viscosity fluid 2. Fluid 1 with low viscosity is introduced in x-direction with fully developed velocity profile and displaces Fluid 2 from channel. During this displacement process the viscous finger gets developed and produces a steady state shape (constant finger tip velocity) as shown in Figure 4.

Average velocity of the inlet fluid 1 is U_1. Viscosity ratio $M = \mu_2/\mu_1$ is 20 which is generally experienced during water flooding process where water displaces oil. No-slip boundary conditions are applied at the channel walls in y-direction whereas velocity inlet and pressure outlet boundary conditions are applied in x-direction. Densities of fluid 1 and 2 have been chosen equal ($\rho_1 = \rho_2 = \rho$) for the simplicity as the density ratio does not affect the finger formation and

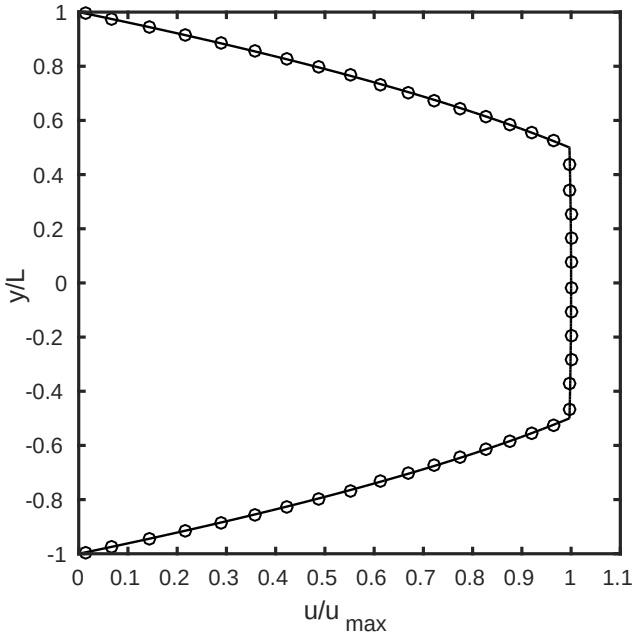

Figure 2: Analytical (−) and numerical (○) velocity profiles for $M = 100$ and $S_w = 0.5$.

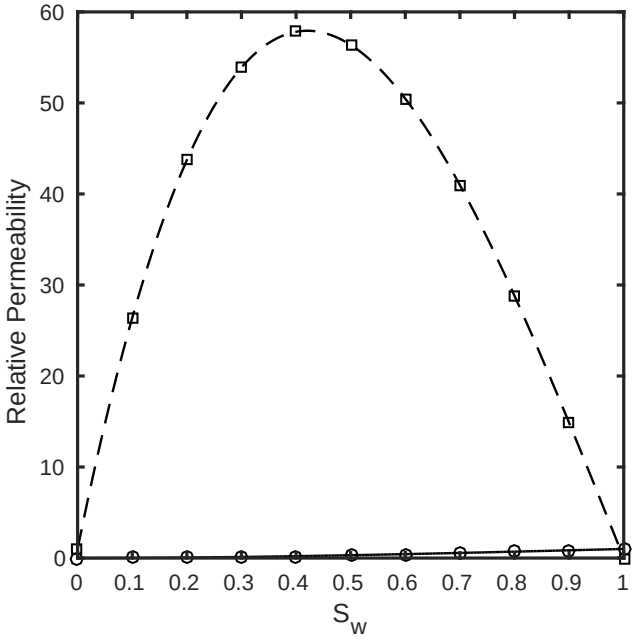

Figure 3: Relative permeability with S_w for $M = 100$: analytical $k_{r,w}$ (−), numerical $k_{r,w}$ (○), analytical $k_{r,nw}$ (−−) and numerical $k_{r,nw}$ (□).

its properties. Capillary and Reynolds number defined using the steady state finger tip velocity U_t are $Ca = \mu_2 U_t/\sigma$ and $Re = \rho U_t H/\mu_2$. From the mass balance, one can find $U_t = U_1 H/W$. To maintain the flow in Stokes regime, value of Ca and Re have been chosen such that $ReCa = 10^{-3}$.
Simulations have been performed with different Ca ranging from 0.025 to 3 with 64 grid cells across the height H. The steady state finger width W and finger tip radius R have been obtained. Figure 5 compares the same finger characteristics parameters in dimensionless form with the results obtained using boundary element method by Halpern and Gaver (1994). Our results of W/H show an excellent match with maximum deviation to be less than 2%. Also, R/H shows an excellent match at low Ca. However at higher Ca, deviation is higher due to higher tip curvatures.

Contact Force Calculation

In this section, we present the grid independence study for contact force at three phase contact line in 3D. Initially, an oil droplet of equivalent radius $R_{eq} = 1$ mm (Volume $V = \frac{4}{3}\pi R_{eq}^2$) is placed on the solid sphere of radius $R_s = 1$ mm such that it inscribes $\theta = 60°$ as shown in Figure 6. In this position,

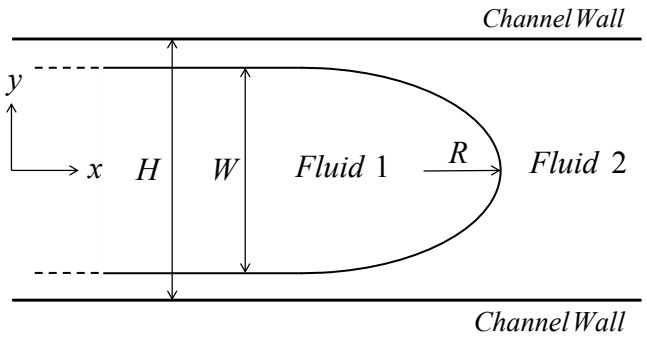

Figure 4: Schematic diagram of steady state viscous finger in 2D channel.

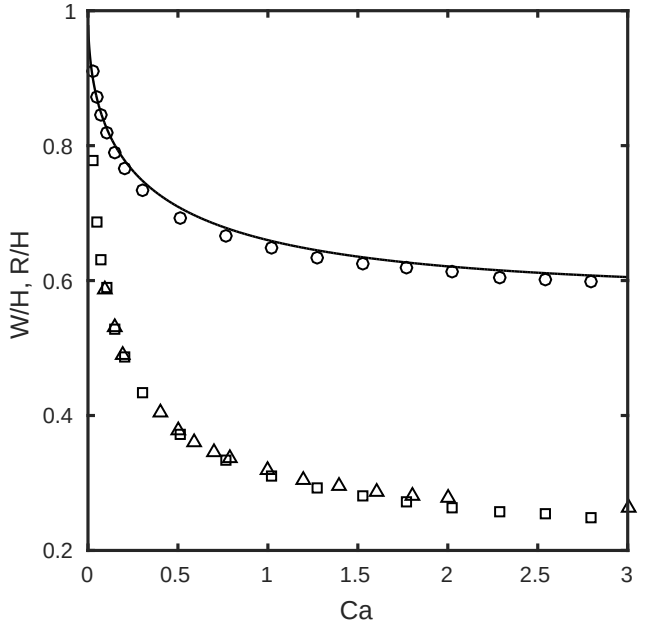

Figure 5: Dimensionless characteristics parameters of steady state viscous finger in 2D channel with Ca a) finger width W/H: present (○), Halpern and Gaver (1994) (−) b) finger tip radius R/H: present (□), Halpern and Gaver (1994) (△).

droplet radius $R_d = 1.1082 R_{eq}$, contact radius $R_c = 0.9069 R_{eq}$ and $\psi = 35.08°$ (Patel *et al.*, 2017). The oil droplet is surrounded by water with $\sigma = 0.03$ N/m. Using a force balance, contact force can be given by following expression,

$$F_{y,analytical} = 2\pi\sigma R_c \sin\psi$$
$$F_{x,analytical} = F_{z,analytical} = 0 \qquad (8)$$

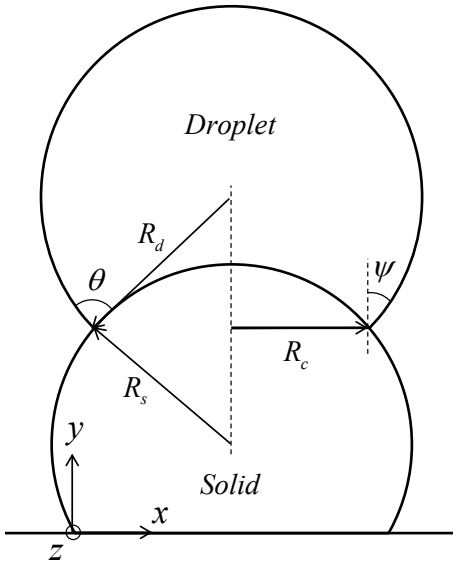

Figure 6: Schematic diagram of droplet on solid sphere for contact force calculation (xy cross section).

Numerical values of the contact force in all three directions have been calculated using the method proposed by Washino *et al.* (2013). The relative error in the contact force in the y-direction is given by following expression,

$$Error\,(\%) = \frac{|F_{y,analytical} - F_{y,numerical}|}{F_{y,analytical}} \times 100\% \qquad (9)$$

Figure 7 shows the relative error in the contact force in y-direction with different grid resolutions. It follows a 1^{st} order trend. However, even at lower grid resolution $(R_c/\Delta \approx 5)$ the relative error is lower than 4%. Moreover, the maximum value of the numerical contact forces in $x-$ and $z-$directions (F_x/F_y and F_z/F_y) is less than 10^{-6} which affirms the accuracy of present coupled IBM-VOF implementation.

RESULTS

In this section, we present pore-scale simulations of a water flooding process such as encountered in enhanced oil recovery. Our aim is to investigate the wettability effects on the mobility of oil through oil-wet and neutrally-wet rocks.
The physical properties of an oil-water system are: $\mu_{oil} = 0.02$ Pa·s, $\mu_{water} = 0.001$ Pa·s, $\rho_{water} = \rho_{oil} = 1000$ kg/m^3 and $\sigma = 0.03$ N/m. Initial distribution of oil and water phases in homogeneous configuration of spheres (rock structure) is shown in Figure 8a. Saturation of oil $S_{oil} = 0.5$ and structure porosity $\phi = 0.5$. Wettability is altered by varying θ for oil-wet $(\theta < 90°)$ and neutrally-wet $(\theta = 90°)$ rocks.
Simulations are performed on a 3D periodic domain with $100\times100\times100$ grid cells of size $\Delta = 1.5\times10^{-5}$ m. In this case, the number of grid cells across the radius of the sphere is around 39 which is quite sufficient to resolve accurate contact force. A constant body force of 10^5 N/m^3 is applied in

x-direction to both oil and water phases. Superficial velocities of both phases are monitored to decide if the flow has reached steady state. Figure 9 shows the plot of superficial velocity of oil U_{oil} with time for oil-wet rocks with $\theta = 45^\circ$. One can observe that U_{oil} repeats itself after a fixed time interval and hence the flow has reached (pseudo) steady state. A snapshot of this (pseudo) steady state is presented in Figure 8b. Using the time averaged superficial velocity of oil $\bar{U}_{oil}$, one can calculate Re, Ca and $k_{r,oil}$ by means of the following expressions,

$$Re = \frac{\rho_{oil}\bar{U}_{oil}D}{\mu_{oil}}$$
$$Ca = \frac{\mu_{oil}\bar{U}_{oil}}{\sigma} \qquad (10)$$
$$k_{r,oil} = \frac{\bar{U}_{oil}(S_{oil})}{\bar{U}_{oil}(S_{oil}=1)}$$

where D is the diameter of sphere and $\bar{U}_{oil}(S_{oil})$ is $\bar{U}_{oil}$ at given S_{oil}. Maximum value of Re and Ca numbers among all simulations are 0.5 and 0.006 respectively ensuring the flow in the Stokes regime.

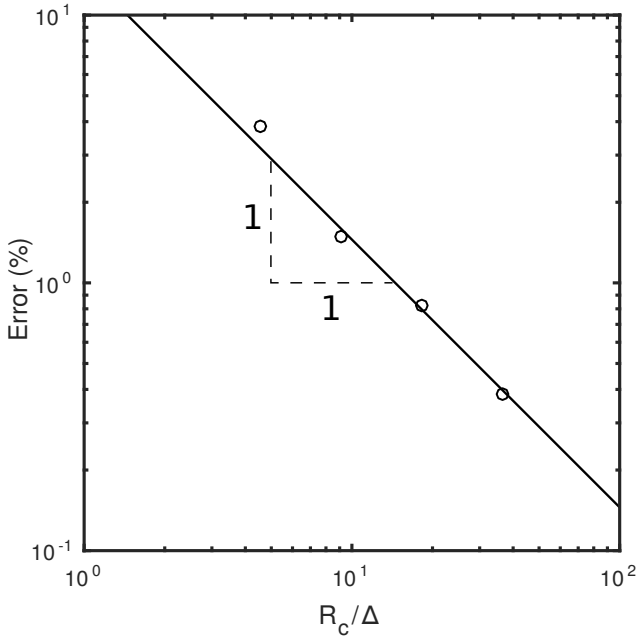

Figure 7: Grid independence study for contact force in y-direction: present (○) and 1^{st} order line (−) for reference

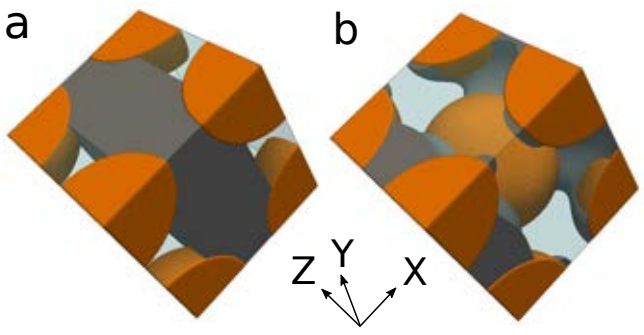

Figure 8: (a) Initial and (b) (pseudo) steady state fluid phase distribution for oil-wet rocks with $\theta = 45^\circ$, $\phi = 0.5$ and $S_{oil} = 0.5$. Oil, water and rocks are represented by grey, transparent blue and brown color respectively.

Figure 10 shows the $k_{r,oil}$ with θ for oil-wet $(\theta < 90^\circ)$ and neutrally-wet $(\theta = 90^\circ)$ rocks. Oil is more mobile in the neutrally-wet rocks as oil and water both have equal wettability towards rocks. As the rocks become more and more oil-wet ($\theta \to 0^\circ$), the tendency of oil to adhere with rocks increases and hence its mobility decreases. Interestingly, this decrement is non-linear and it may fully choke the flow at a lower body force. The maximum difference in $k_{r,oil}$ compared to its mean value is around 50% which suggests that the wettability has a strong effect on the oil recovery during water flooding process.

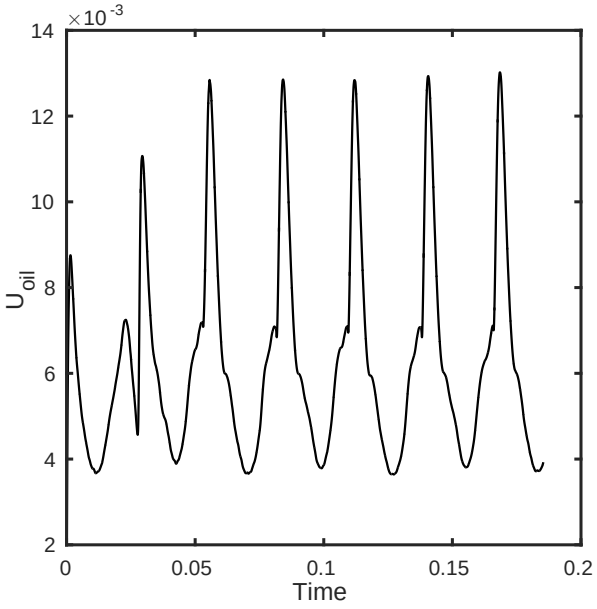

Figure 9: U_{oil} with time for oil-wet rocks with $\theta = 45^\circ$, $\phi = 0.5$ and $S_{oil} = 0.5$.

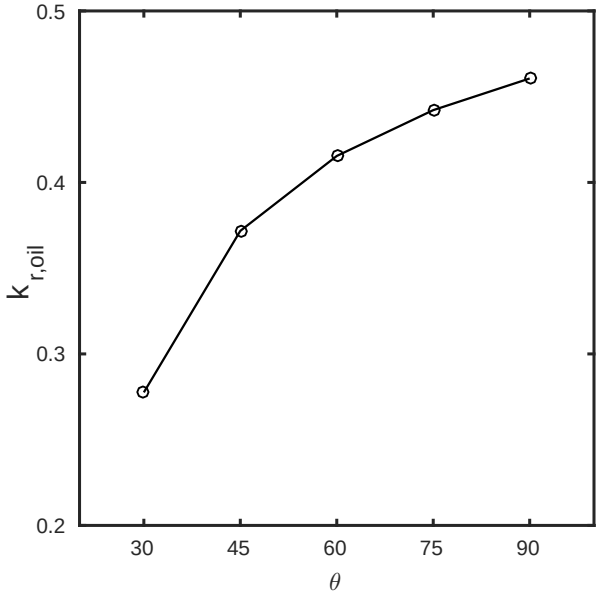

Figure 10: $k_{r,oil}$ with θ for oil-wet $(\theta < 90^\circ)$ and neutrally-wet $(\theta = 90^\circ)$ rocks with $\phi = 0.5$ and $S_{oil} = 0.5$

CONCLUSION

In this paper a methodology is presented to simulate the multiphase flows involving oil and water from complex geometries. IBM is used to simulate the dynamic interactions between fluids and complex geometries on a Cartesian computational grid. Present IBM is second order, direct forcing, implicit and doesn't require any calibration for different geometries. Sharp interface VOF method is used to track multi-fluid interfaces. IBM and VOF are coupled at the three phase contact line via the apparent contact angle. Present methodology works perfectly well for the validation/verification test cases involving oil-water flows and yields more accurate results compared to simulations performed using the Lattice-Boltzmann method. Pore-scale water flooding simulations are presented to quantify the effect of wettability on the mobility of oil through oil-wet and neutrally-wet homogeneous rocks. Obtained results show that the oil-wet rocks can drastically reduce the mobility of oil.

In future, this work will be continued on large randomized structures with number of spheres in order of 100 to quantify the effect of wettability, porosity, capillary number, saturation, viscosity ratio etc. on the mobility of oil-water flows.

ACKNOWLEDGMENTS

This work is part of the Industrial Partnership Program (IPP) 'Computational sciences for energy research' of the Foundation for Fundamental Research on Matter (FOM), which is part of the Netherlands Organization for Scientific Research (NWO). This research program is co-financed by Shell Global Solutions International B.V.

REFERENCES

BRACKBILL, J.U., KOTHE, D.B. and ZEMACH, C. (1992). "A continuum method for modeling surface tension". *Journal of computational physics*, **100(2)**, 335–354.

DAS, S., DEEN, N.G. and KUIPERS, J.A.M. (2016). "Immersed boundary method (ibm) based direct numerical simulation of open-cell solid foams: Hydrodynamics". *AIChE Journal*.

DEEN, N.G., KRIEBITZSCH, S.H.L., VAN DER HOEF, M.A. and KUIPERS, J.A.M. (2012). "Direct numerical simulation of flow and heat transfer in dense fluid–particle systems". *Chemical engineering science*, **81**, 329–344.

HALPERN, D. and GAVER, D.P. (1994). "Boundary element analysis of the time-dependent motion of a semi-infinite bubble in a channel". *Journal of Computational Physics*, **115(2)**, 366–375.

HIRT, C.W. and NICHOLS, B.D. (1981). "Volume of fluid (vof) method for the dynamics of free boundaries". *Journal of computational physics*, **39(1)**, 201–225.

HUANG, H. and LU, X.Y. (2009). "Relative permeabilities and coupling effects in steady-state gas-liquid flow in porous media: A lattice boltzmann study". *Physics of Fluids*, **21(9)**, 092104.

MITTAL, R. and IACCARINO, G. (2005). "Immersed boundary methods". *Annu. Rev. Fluid Mech.*, **37**, 239–261.

PATEL, H.V., DAS, S., KUIPERS, J.A.M., PADDING, J.T. and PETERS, E.A.J.F. (2017). "A coupled volume of fluid and immersed boundary method for simulating 3d multiphase flows with contact line dynamics in complex geometries". *Chemical Engineering Science*, **166**, 28–41.

PROSPERETTI, A. (2002). "Navier-stokes numerical algorithms for free-surface flow computations: An overview". *Drop-Surface Interactions*, 237–257. Springer.

SHENG, J.J. (2014). "Critical review of low-salinity waterflooding". *Journal of Petroleum Science and Engineering*, **120**, 216–224.

SNOEIJER, J.H. and ANDREOTTI, B. (2013). "Moving contact lines: scales, regimes, and dynamical transitions". *Annual review of fluid mechanics*, **45**, 269–292.

VAN SINT ANNALAND, M., DEEN, N.G. and KUIPERS, J.A.M. (2005). "Numerical simulation of gas bubbles behaviour using a three-dimensional volume of fluid method". *Chemical Engineering Science*, **60(11)**, 2999–3011.

WASHINO, K., TAN, H.S., HOUNSLOW, M.J. and SALMAN, A.D. (2013). "A new capillary force model implemented in micro-scale cfd–dem coupling for wet granulation". *Chemical Engineering Science*, **93**, 197–205.

WÖRNER, M. (2003). *A compact introduction to the numerical modeling of multiphase flows*. Forschungszentrum Karlsruhe.

YIOTIS, A.G., PSIHOGIOS, J., KAINOURGIAKIS, M.E., PAPAIOANNOU, A. and STUBOS, A.K. (2007). "A lattice boltzmann study of viscous coupling effects in immiscible two-phase flow in porous media". *Colloids and Surfaces A: Physicochemical and Engineering Aspects*, **300(1)**, 35–49.

YOUNGS, D.L. (1982). "Time-dependent multi-material flow with large fluid distortion". *Numerical methods for fluid dynamics*, **24(2)**, 273–285.